Quasi-nonvolatile storage in Ru-doped $Bi_{12}SiO_{20}$ crystals by two-wavelength holography

Vera Marinova,[1*] Ren Chung Liu,[1] Shiuan Huei Lin,[2,3] and Ken Yuh Hsu[1]

[1]*Department of Photonics, National Chiao Tung University, University Str., 1001, Hsinchu 30050, Taiwan*
[2] *Department of Electrophysics, National Chiao Tung University, University Str., 1001, Hsinchu 30050, Taiwan*
[3]*lin@cc.nctu.edu.tw*
[*]*veramarinova@nctu.edu.tw*

Abstract: Prolonged read-out process of a hologram recorded at near infrared with simultaneous green light exposure is measured in Ru-doped $Bi_{12}SiO_{20}$ crystal. The experimental results are confirmed by numerical simulations, suggesting two different traps involved in the space-charge transport mechanism. In addition, quasi-permanent holographic recording of image with fast updating speed by using two-wavelength recording is demonstrated.

OCIS codes: (090.5694) Real-time holography; (160.5320) Photorefractive materials.

References and links

1. J. J. Amodei and D. L. Steabler, "Holographic pattern fixing in electro-optic crystals," Appl. Phys. B **18**, 540–542 (1971).
2. F. Micheron and G. Bismuth, "Electrical control of fixation and erasure of holographic patterns in ferroelectric materials," Appl. Phys. Lett. **20**(2), 79–81 (1972).
3. K. Buse, A. Adibi, and D. Psaltis, "Non-volatile holographic storage in doubly doped lithium niobate crystals," Nature **393**(6686), 665–668 (1998).
4. J. Frejlich, *Photorefractive Materials* (Wiley Interscience, 2007).
5. M. P. Georges, V. S. Scauflaire, and P. C. Lemare, "Compact and portable holographic camera using photorefractive crystals. Application in various metrological problems," Appl. Phys. B **72**(6), 761–765 (2001).
6. E. A. Barbosa, A. O. Preto, D. M. Silva, J. F. Carvalho, and N. I. Morimoto, "Denisiuk-type reflection holography display with sillenite crystals for imaging and interferometry of small objects," Opt. Commun. **281**(3), 408–414 (2008).
7. G. Caroena, M. Mori, M. R. R. Gesualdi, E. A. Liberti, E. Ferrara, and M. Muramatsu, "Mastication effort study using photorefractive holographic interferometry technique," J. Biomech. **43**(4), 680–686 (2010).
8. S. G. Odoulov, K. V. Shcherbin, and A. N. Shumeljuk, "Photorefractive recording in BTO in the near infrared," J. Opt. Soc. Am. B **11**(9), 1780–1785 (1994).
9. P. V. dos Santos, J. Frejlich, and J. F. Carvalho, "Direct near infrared photorefractive recording and pre-exposure controlled hole-electron cometition with enhanced recording in undoped $Bi_{12}TiO_{20}$," Appl. Phys. B **81**(5), 651–655 (2005).
10. E. Raita, O. Kobozev, A. A. Kamshilin, and V. V. Prokofiev, "Fast photorefractive response in $B_{12}SiO_{20}$ in the near infrared," Opt. Lett. **25**(17), 1261–1263 (2000).
11. V. Marinova, M. L. Hsieh, S. H. Lin, and K. Y. Hsu, "Effect of ruthenium doping on the optical and photorefractive properties of $Bi_{12}TiO_{20}$ single crystals," Opt. Commun. **203**(3-6), 377–384 (2002).
12. V. Marinova, S. H. Lin, V. Sainov, M. Gospodinov, and K. Y. Hsu, "Light-induced properties of Ru-doped $Bi_{12}TiO_{20}$ crystals," J. Opt. A, Pure Appl. Opt. **5**(6), S500–S506 (2003).
13. F. Ramaz, L. Rakitina, M. Gospodinov, and B. Briat, "Photorefrcative and photochromic properties of ruthenium –doped $Bi_{12}SiO_{20}$," Opt. Mater. **27**(10), 1547–1559 (2005).
14. V. Marinova, R. C. Liu, S. H. Lin, and K. Y. Hsu, "Real-time holography in ruthenium-doped bismuth sillenite crystals at 1064 nm," Opt. Lett. **36**(11), 1981–1983 (2011).
15. P. Sveshtarov and M. Gospodinov, "The effect of the interface shape on authomatic Czochralski weight diameter control system performance," J. Cryst. Growth **113**(1-2), 186–208 (1991).
16. R. Oberschmid, "Absorption Centers of $Bi_{12}GeO_{20}$ and $Bi_{12}SiO_{20}$ crystals," Phys. Stat. Solidi A **89**(1), 263–270 (1985).
17. I. Ahmad, V. Marinova, and E. Goovaerts, "High-frequency electron paramagnetic resonance of the hole trapped anti-site bismuth centre in the photorefractive bismuth sillenite crystals," Phys. Rev. B **79**(3), 033107 (2009).
18. V. Marinova, I. Ahmad, and E. Goovaerts, "Dynamics of charge carriers in Ru-doped $Bi_{12}SiO_{20}$ crystals after ns laser pulse excitation," J. Appl. Phys. **107**, 113106 (2010).

#169361 - $15.00 USD Received 29 May 2012; revised 18 Jul 2012; accepted 25 Jul 2012; published 13 Aug 2012

19. N. V. Kukhtarev, V. B. Markov, S. G. Odulov, M. S. Soskin, and V. L. Vinetskii, "Holographic storage in electro-optic crystals I. Steady state," Ferroelectrics **22**(1), 949–960 (1978).
20. J. Imbrock, D. Kip, and E. Krätzig, "Nonvolatile holographic storage in iron-doped lithium tantalate with continuous-wave laser light," Opt. Lett. **24**(18), 1302–1304 (1999).
21. A. Adibi, K. Buse, and D. Psaltis, "Two-center holographic recording," J. Opt. Soc. Am. B **18**(5), 584–601 (2001).

1. Introduction

Several approaches such as thermal fixing [1], electrical fixing [2] and two-color recording [3] have been developed to overcome the volatility problem during the holographic read-out processes and to prolong the grating life-time of different photorefractive materials. Among them the two-color (or photon-gated) holographic recording is regarded as the most attractive and challenging technique because of the all optical processing in real time and in situ. Nowadays it is of practical importance to implement the two-color holography at practically feasible near infrared (NIR) wavelengths owing to the low cost and low-power diode lasers availability. Therefore it is of special importance to improve the near infrared sensitivity, response time and at the same time to prolong the recorded grating lifetime of different photorefractive materials, which can be used for real-time updatable memories, accurate non-invasive biomedical image testing and further applications.

Sillenite type crystals are known as one of the best inorganic materials for real-time image processing and related dynamic applications, especially for non-destructive interferometric testing [4–7]. In a past, special efforts have been made to optimize the sillenite's properties at NIR spectral range. Photosensitivity improvement and beam-coupling coefficient enhancement in un-doped $Bi_{12}TiO_{20}$ (BTO) after pre-exposure or simultaneous exposure with visible light has been reported by Odulov *et al.* [8]. Later on, improved NIR recording and extended lifetime has been achieved in un-doped BTO due to the hole-based complementary grating after green light pre-exposure [9]. At the same time, a modification of sillenite's structure by reduction/oxidation treatments [10] or by adding suitable dopants have been done [11,12]. For example, Ru addition shows prospective features for energy transfer and two-beam coupling efficiency enhancement [13]. Recently, we found that Ru is an excellent dopant in sillenites which improves the photosensitivity and response-time of 60 ms at 1064 nm is detected after green light pre-excitation [14].

In the present work, the possibility to prolong the read-out process in Ru-doped BSO at 1064 nm by using two-wavelength recording is demonstrated and confirmed by numerical simulations. In addition, quasi-permanent image reconstruction experiment is presented to support the extended life-time.

2. Experimental

Fully faceted Ru-doped BSO crystals with excellent optical quality have been obtained by the Czochralski growth method [15]. Ruthenium concentration of 6.1×10^{18} cm^{-3} in the grown crystal was determined by atomic absorption spectrometry.

For holographic experiments, cube with rectangular dimensions 10.3 x 11.4 x 6.4 mm along (110), (1-10) and (001) crystallographic directions was prepared. Two-beam interference set-up in transmission geometry was used for holographic recording by using diode-pumped laser operating at 1064nm. The intensity of each recoding beam was about 110 mW/cm^2 and 30° of the writing angle outside the crystal. Verdi laser (532nm with adjustable power) was used as gating light during the recording process, and turn off during the read-out. The holographic grating was probed in real-time by the third beam, coming from additional diode laser at 1064nm with low intensity. Sample was thermally annealed before the experiments. For the image reconstruction test demonstration, the signal beam carried the magnified image of the mask, which first was stored in the Ru-doped BSO crystal (with IR light only or 1064nm simultaneously with 532nm) and afterwards reconstructed by the 1064

#169361 - $15.00 USD Received 29 May 2012; revised 18 Jul 2012; accepted 25 Jul 2012; published 13 Aug 2012

nm reference beam. The image quality evolution in time was detected by the CCD camera (640 x 480 pixels).

3. Results and discussions

Figure 1 shows comparison between recording and erasure behavior when 1064nm wavelength is used for the recording (IR only) and when simultaneously 1064nm and 532nm (with different intensities) are used for the recording. As it seen once the crystal is irradiated simultaneously with green light, an improvement of the recording speed is achieved. The recording process begins with fast growth during the first few tens of ms, followed by slightly decrease of the diffracted beam intensity after prolonged time of the recording. The read-out (after 3.2s) starts with fast decay in the beginning, followed by slow decrease of the diffracted beam intensity when the gating intensity is weak (< 10 mW/cm^2). The diffracted signal even becomes oscillating as the pump intensity increases and the grating persists for longer life time.

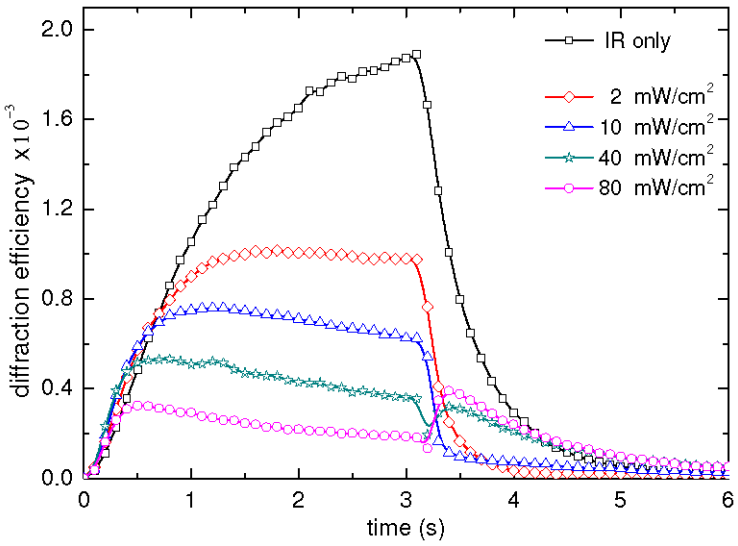

Fig. 1. Holographic dynamics of the recording and read-out processes of BSO:Ru crystal using 1064 nm for recording (IR only) and simultaneously 1064 nm + 532 nm (different pump intensity during the recording). The read-out process is performed at 1064 nm.

Optically pumping the electrons with gating light is recognized method to enhance the near-infrared properties of sillenites [8]. Some authors assigned the observed transient character during holographic recording to simultaneous electron-hole gratings competition [9,10]. Generally, the anti-site Bi defect (known as $Bi^{3+}_{Si} + h$ center upon illumination assuming n-type photoconductivity), is identified as the main photorefractive defect in sillenite structure. This anti-site Bi defect is connected to the Bi^{3+}/Bi^{4+} donor level (located at 2.2 eV below the conduction band (CB) at room temperature [16] and is recognized as a key source of photoelectrons for photorefractive and related light-induced effects. Ruthenium as transition metal ion can occur in several valence states whereas some of them may appear only after appropriate light excitation. First Ramaz *et al.* [13] using magnetic circular dichroism demonstrated that Ru^{n+} substitute Bi-sites in pseudo-octahedron position under three valence states: Ru^{4+} can accept holes or electrons to produce Ru^{5+} or Ru^{3+}, respectively due to it's amphotetic behavior. Further electron paramagnetic resonance direct detection proved that Ru doping results in ($Bi^{3+}_{Si} + h$) center already in the as-grown crystal and Ru introduces electron accepting levels close to the valence band (VB) [17]. Recently, photo-induced absorption study reveal an evidence of Ru-related high density of trap levels

#169361 - $15.00 USD Received 29 May 2012; revised 18 Jul 2012; accepted 25 Jul 2012; published 13 Aug 2012

(positioned more shallow than the deep levels typical for sillenites), acting as acceptor centers for photoexcited electrons [18]. Based on above results and detected broad absorption peak after green light pre-excitation [14], we suppose that Ru addition introduce trap centers, which are located more shallow than the main photorefractive level at 2.2 eV.

In order to analyze the experimental results presented at Fig. 1 we assume two kinds of trap centers: deep traps (from where the charge carriers are excited by 523nm) and shallow traps (which are sensitive to 1064nm). The observed dynamic behavior can be described by the set of nonlinear coupled equations, which has been proposed by A. Adibi for optical fixing in doubly-doped $LiNbO_3$ crystals [19]. It is modified Kukhtarev band transport model [20] by adding one more electron rate equation (Eq. (2)) for the second trap center:

$$\frac{dN_1^+}{dt} = (N_1 - N_1^+)(s_{11}I_1 + \beta_1) - \gamma_1 N N_1^+ \tag{1}$$

$$\frac{dN_2^+}{dt} = (N_2 - N_2^+)(s_{21}I_1 + s_{22}I_2 + \beta_2) - \gamma_2 N N_2^+ \tag{2}$$

$$\frac{dN}{dt} = \frac{dN_1^+}{dt} + \frac{dN_2^+}{dt} + \frac{1}{e}\frac{dJ}{dz} \tag{3}$$

$$J = e\mu NE + \mu k_B T \frac{dN}{dz} \tag{4}$$

$$\varepsilon \frac{dE}{dz} = e(N_1^+ + N_2^+ - N - N_A) \tag{5}$$

(all parameters physical meanings are presented in Fig. 2 captions). Following the procedure of linearization (for small modulation depth m of interference fringe), we assume the following forms:

$$N_1^+ = N_{10}^+ + N_{11}^+ \cos(Kz) \tag{6}$$

$$N_2^+ = N_{20}^+ + N_{21}^+ \cos(Kz) \tag{7}$$

$$N = N_0 + N_1 \cos(Kz) \tag{8}$$

$$J = J_0 + J_1 \cos(Kz) \tag{9}$$

$$E = E_0 + E_{SC} \cos(Kz) \tag{10}$$

We first substitute the Eqs. (6)–(10) into Eqs. (1)–(5), where the equations for the zero – and first order terms are expressed as:

$$\frac{dN_{10}^+}{dt} = \left(N_1 - N_{10}^+\right) g_1 - \gamma_1 N_0 N_{10}^+ \tag{11}$$

$$\frac{dN_{20}^+}{dt} = \left(N_2 - N_{20}^+\right) g_2 - \gamma_2 N_0 N_{20}^+ \tag{12}$$

where: $g_1 = s_{11}I_{10} + \beta_1; g_2 = s_{21}I_{10} + s_{22}I_{20} + \beta_2; N_0 = N_{10}^+ + N_{20}^+ - N_A$

$$\frac{dN_{11}^+}{dt} = -\left(g_1 + \gamma_1 N_0\right) N_{11}^+ - \gamma_1 N_{10}^+ N_1 \tag{13}$$

#169361 - $15.00 USD Received 29 May 2012; revised 18 Jul 2012; accepted 25 Jul 2012; published 13 Aug 2012

$$\frac{dN_{21}^{+}}{dt} = -\left(g_2 + \gamma_2 N_0\right) N_{21}^{+} - \gamma_2 N_{20}^{+} N_1 + mS_{22} I_{20}\left(N_2 - N_{20}^{+}\right) \tag{14}$$

$$\begin{aligned} \frac{dN_1}{dt} = & \left(-\frac{K^2 \mu k_B T}{e} - \frac{e\mu N_0}{\varepsilon} - \gamma_1 N_{10}^{+} - \gamma_2 N_{20}^{+} \right) N_1 + \\ & + \left(\frac{e\mu N_0}{\varepsilon} - g_1 - \gamma_1 N_0 \right) N_{11}^{+} + \left(\frac{e\mu N_0}{\varepsilon} - g_2 - \gamma_2 N_0 \right) N_{21}^{+} + mS_{22} I_{20}\left(N_2 - N_{20}^{+}\right) \end{aligned} \tag{15}$$

$$E_{SC} = -i\,\frac{e}{\varepsilon K}\left(N_{11}^{+} + N_{21}^{+} - N_1\right) \tag{16}$$

These equations are solved with the following assumption for exciting I_1 and recording I_2 laser beam intensities:

$$I_1 = \begin{cases} I_{10}, \text{ at recording stage} \\ 0, \text{at read-out stage} \end{cases} \quad \text{and} \quad I_2 = \begin{cases} I_{20}(1 + m\cos Kz), \text{ at recording stage} \\ I_{20}, \text{at read-out stage} \end{cases} \tag{17}$$

In these terms, for high conductivity in Ru-doped BSO, the rate of the zero-order terms N_{10}^{+}, N_{20}^{+} and N change towards their steady-state values with almost the same rate of the first-order terms N_{11}^{+}, N_{21}^{+} and N_1. Therefore, there is no analytical solution and we solve numerically the set of Eqs. (1)-(5) by first calculating the temporal evolution of the zero-order terms and substitute them into first order equations. Then using these temporal curves we solve the temporal evolution of E_{SC} (Eq. (16)) at both recording and erasure stages (the refractive index modulation is proportional to the E_{SC} temporal evolution).

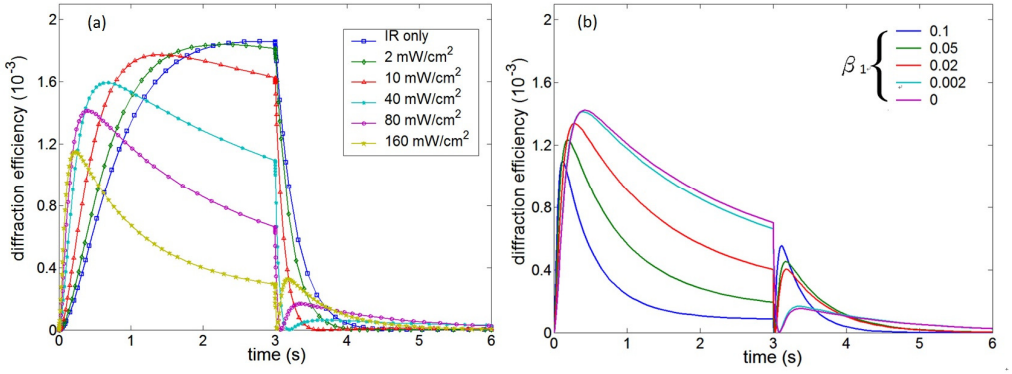

Fig. 2 .(a) Theoretical simulation results and some parameter values: ε-dielectric constant; μ-carrier mobility 2.5x10−6 (m2/Vs); e-electron charge 1.6x10−19 (C); K-grating vector 6.11 (μm−1); NA-density of acceptor 1.0 x1024 (m−3); N1- density of deep traps 2.0x1024 (m−3); N2 -density of shallow traps 1.0x1024 (m−3); N+1-density of ionized deep traps (m−3); N+2 -density of ionized shallow traps (m−3); N-charge carrier density in the conduction band (m−3); S11- photo-ionization cross section of deep trap 1.2x10−4 (m3/J) at shorter wavelength; S21-photo-ionization cross section of shallow trap 3.56x10−4 (m3/J) at shorter wavelength; S22-photo-ionization cross section of shallow trap 0.3x10−4 (m3/J) at longer wavelength; J-current density (A/m2); γ1(m3/s)- recombination rate constant of deep trap 5.0x10−18; γ2(m3/s)-recombination rate constant of shallow trap 3.0x10−16; β1-thermal generation rate constant of deep trap (up to 0.002 (s−1)); β 2 -thermal generation rate constant of shallow trap 0.2 (s−1); r-electro-optic coefficient 2.25x10−12 (m/V); Esc-space charge field; (b) Temporal evolution of diffracted signal at both recording and read-out processes at different thermal generation rates β1 [s−1] the intensity of gating light is 80 mW/cm2.

#169361 - $15.00 USD Received 29 May 2012; revised 18 Jul 2012; accepted 25 Jul 2012; published 13 Aug 2012

Performed theoretical simulations data are presented at Fig. 2(a). As it seen, the oscillation of the temporal response becomes larger in both recording and read-out stages as the intensity of exciting beam increases, which almost fits qualitatively with the observed experimental results. Since there is more than one unknown parameter, we do not attempt to fit the experimental curve quantitatively. The diffraction efficiency values do not follow exactly the experimental one (shown at Fig. 1) since we do not take into account the absorption coefficient during the theoretical simulation.

However, an important remark which comes out from the performed theoretical calculation must be noticed: using a gating light during holographic recording, two complementary space charge gratings result from two different traps, localized at Ru-doped BSO structure. The existence of two different traps is usually considered as a reason for the non-volatile photorefractive grating in doped $LiNbO_3$ crystals as well [3, 19, 21]. Although similar nonlinear coupled equations model explained the results for $LiNbO_3$ and BSO, the observed oscillating behavior in BSO can be assigned to the higher charge carrier mobility and higher thermal generation rate constants, which play significant role for hologram stabilization (material with low thermal generation rate is required for optical fixing) and cannot be neglected during performed theoretical simulation. Furthermore, the lack of bulk photovoltaic effect in sillenite structure, which is relevant for the efficiency of fixed holograms in non-centro symmetric crystals as $LiNbO_3$ is crucial. Numerical results on thermal generation rate β_1 influence on grating persistence are shown at Fig. 2(b).

As it seen, the thermal generation rate of deep trap β_1 strongly influents the temporal evolution of the diffracted signal, meanwhile prolonged read-out process is detected as the thermal generation rate decreases. As a result, persistence of photorefractive hologram against the uniform read-out beam becomes saturated when β_1 is small enough. It indicates that the key issue for achieving optical fixing in Ru-doped BSO is to growth the crystal with very low thermal generation rate. It is also a sign that holographic properties of BSO:Ru at near infrared can be tailored by introducing multiple trap centers and suitable gating light. However, more careful investigations of the influences of crystal parameters are necessary in order to accomplish the desired response in practical applications.

Figure 3 shows comparison of the reconstructed image evolution, recorded in BSO:Ru (thermally annealed sample) for 5s using: single IR light (a-c) and two-wavelength recording (d-f). Obviously, by two-wavelength recording the image quality can be kept longer time. The last two rows show example of fast updating speed and reversibility of Ru-doped BSO, displaying two images ("NCTU" and "中山), recorded at the same crystal location. First, Fourier hologram of "NCTU" is recorded simultaneously with 1064nm + 532nm. Immediately after the image becomes stable, the "NCTU" mask is replaced with "中山'image which is recorded with single IR light at the same crystal location. As it seen, at the beginning of the reconstruction process both images appear simultaneously (g), followed by quick erasure of "中山' (h) (recorded with single IR), while "NCTU" image (recorded by 1064nm + 532nm) still remains in a good quality (i). Afterward, "NCTU" is completely erased by green light illumination. The "中山' image is recorded again in the same location (j), by two-wavelength simultaneously. The last figure displays the "中山' image time evolution, which show very good quality (k) and it is stable more than 1 min.

#169361 - $15.00 USD Received 29 May 2012; revised 18 Jul 2012; accepted 25 Jul 2012; published 13 Aug 2012

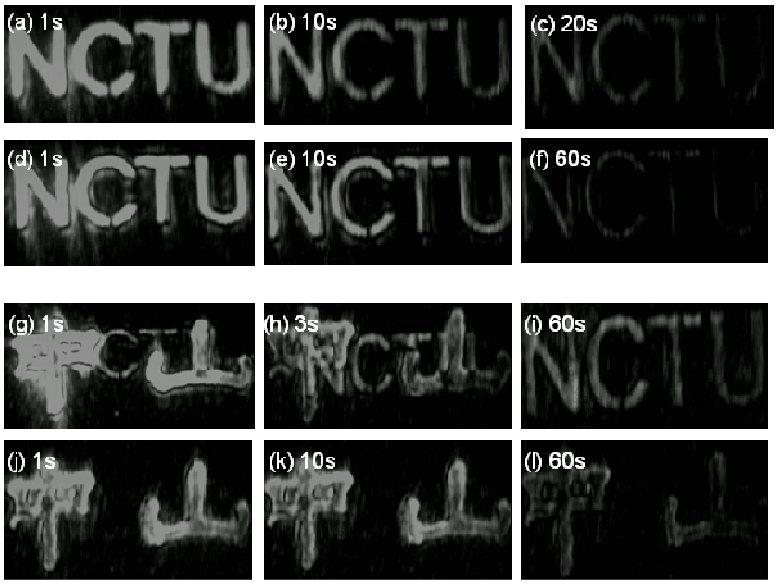

Fig. 3. Time evolution of reconstructed image recorded with: (a-c) IR light only; (d-f) 1064nm + 532nm. Last two rows: (g-i) "NCTU" recorded with 1064nm + 532nm, replaced by "中山" recorded with IR only and (j-l) "中山" recorded with 1064nm + 532 nm in the same crystal location after complete erasure of the previous image.

4. Conclusion

In summary, we have demonstrated possibility to extend the holographic grating lifetime in Ru-doped BSO by combining two-wavelength recording. Quasi-permanent storage of image with relatively fast updating speed using low intensity operation at near-infrared and without external electric field is demonstrated. Presented results show perspective future of Ru-doped BSO for further applications in real-time image processing and non-destructive bio-objects testing.

Acknowledgments

Financial support by NSC, Taiwan under contract NSC 101-2911-I-009 –508 and by Ministry of Education, Taiwan under AUT program is gratefully acknowledged. Samples were grown by the Crystal Growth Laboratory, Institute of Solid State Physics, Sofia, Bulgaria.

#169361 - $15.00 USD Received 29 May 2012; revised 18 Jul 2012; accepted 25 Jul 2012; published 13 Aug 2012